

## Recent examples of cathodoluminescence as a probe of surface structure and composition

P. D. TOWNSEND, T. KARALI, A. P. ROWLANDS, V. A. SMITH AND G. VAZQUEZ

School of Engineering, Pevensey Building, University of Sussex, Brighton, BN1 9QH, UK

### ABSTRACT

Cathodoluminescence (CL) provides a sensitive analytical probe of the near-surface region of insulating materials, and some new examples of the strengths of the technique are presented using recent data from the University of Sussex. Analysis of float glass shows that by spectral and lifetime resolved data it is possible to separate the emission bands from excitonic, intrinsic imperfections, and impurities in various valence states, as a function of their depth beneath the surface. Correlation of the CL data with those from Mössbauer, ion beam and other analyses then provides the basis for models of the defect sites. CL from a second glass, ZBLAN, reveals the presence of microcrystallites and growth defects, and the work underpins confidence in the high purity gas levitation method of ZBLAN production. New results on CL of wavelength shifts with crystal field of Mn in carbonates are presented, and of Nd emission from Nd:YAG. The effects are directly linked to surface damage and dislocations caused by sample preparation steps of cutting and polishing. Methods to minimise the damage, by furnace or pulsed laser annealing, and chemical routes, are mentioned. Such surface preparation damage has a profound effect on all CL monitoring, whether for fundamental studies or mineralogical applications. Finally, a route to eliminate such problems is demonstrated, with consequent improvements in luminescence, transmission and laser performance of surface waveguides. The implications of improved surface quality range widely from mineralogical CL imaging through improved photonic materials and epitaxial growth to elimination of surface damage, and additional information.

**KEYWORDS:** cathodoluminescence, surface structure, surface composition, Mössbauer spectroscopy.

### Introduction

CATHODOLUMINESCENCE (CL) is a powerful technique for exciting light emission from intrinsic relaxations, impurities and imperfections in the outer few microns of the surface of insulating (and semiconducting) materials. However, it suffers from a number of problems, such as the fact that the luminescence efficiency is dramatically altered by surface states, dislocations and structural imperfections. It is also quite unselective in the excitation process and so it is essential to make both spectral and time resolution of the light output in order to separate fully the component signals. There are additional confusing factors from defect creation, charge readjustments, current density and heating induced by the electron beam. Whilst recognising that it is not a passive probe of surface states, it

nevertheless has such sensitivity that it can provide information where other surface techniques are inadequate. Consequently it has been a key feature in a variety of recent studies of imperfections in insulators. This review cites some of the new results and indicates how, when used as a complementary technique, it offers significant analytical information.

The examples presented are all from recent or current CL work at the University of Sussex. This rather limited viewpoint is partly for convenience, and partly because the data include some associated thermoluminescence (TL) and radioluminescence (RL) work with the same samples, together with alternative analytical studies, plus applications of CL in materials which have not received detailed study from other research groups. However, the underlying principles and types of information are broadly consistent with

those discussed in other review papers. Considering that CL has been studied for more than a century (Crookes, 1879), there are relatively few CL texts (Marshall, 1988; Pagel *et al.*, 1999; Ozawa 1990; Yacobi and Holt, 1990) and reviews (Remond *et al.*, 1992; Walker and Burley, 1991; Yacobi and Holt, 1986). However, a recent review of luminescence spectral analysis of minerals, particularly TL, includes references to CL, and has an extensive bibliography (Krbetschek *et al.*, 1998).

### Surface analyses of float glass

Spectral analysis is an essential prerequisite for CL, since, as exemplified by the very similar signals obtained from silica glass, crystalline quartz or float glass, there are at least 10 similar emission bands between 300 and 800 nm related to either intrinsic relaxed electron-hole recombination, or intrinsic oxygen defect sites for the silicate structural unit (Agullo Lopez *et al.*, 1988; Stevens-Kalceff and Phillips, 1995; Townsend *et al.*, 1998). The relative intensities, lifetimes and temperature dependencies of the bands differ, and they are modified by thermal processing, and in the changing chemistry of the surface of float glass. They also differ greatly with depth into the surface and between samples. There are additional signals from trace impurities, but the data for float glass, summarised below, demonstrate how one may make detailed separation of the various intrinsic defects, impurities and their mutual interactions, together with changes in the valence states, as a function of depth into the glass. Such information is of value for commercial glass processing when annealing, bending, or application of coating layers is made, or the surface changes during weathering. The changes may be subtle, even where they significantly influence the commercial viability of the glass product, hence any parameter which responds to such changes is helpful, and CL is consistently valuable as a sensitive monitoring tool, even where detailed understanding of the luminescence sites is weak. Nevertheless, from the industrial viewpoint the CL offers a simple monitor of the surface and how it responds to processing. For example there are changes in the CL spectra following heating and glass bending and the formation of an undesirable bloom on the surface (Merbay *et al.*, 1998).

Figure 1 presents examples of room temperature CL spectra and contrasts signals from the

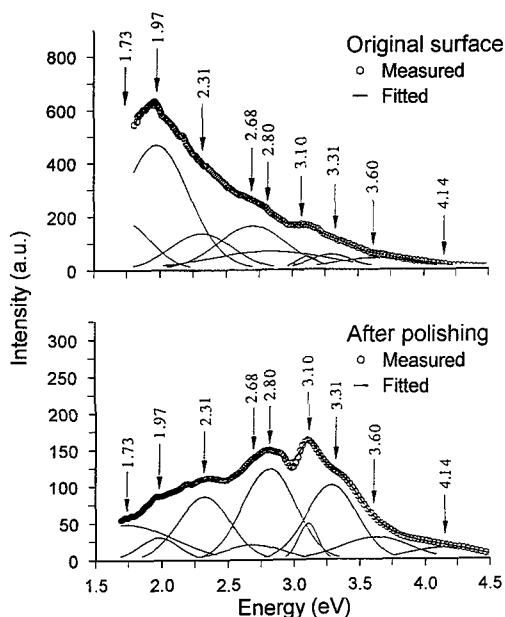


FIG. 1. A comparison of the near surface (upper figure) and interior (lower figure) CL from the tin side of samples of float glass. A deconvolution of the spectra into a set of Gaussian shaped emission bands has been made, and the values shown indicate that at least 9 bands are required.

near surface of float glass, with those from a deeper section obtained by polishing to expose a layer below the zone influenced by tin diffusion from the float bath. The spectral components have been separated by assuming Gaussian shaped emission bands and, despite the rather featureless and overlapping nature of the spectra, the same set of parameters appears to fit most of the data sets from different depths into the tin doped layer. The figure indicates the minimum number of bands which give a close match to the data, but in practice several of the bands are summations of less well defined components. As mentioned, they strongly resemble the signals recorded from CL of silica and quartz (Stevens-Kalceff and Phillips, 1995), as compared in Table 1. Even though nominally the same bands appear at different depths they do not represent a single excitation process, since they differ between samples and display a variety of lifetimes. The Gaussian band fits of Fig. 1 may be used as an indication of the component features, but it is instructive to recognise that between collection of the original

TABLE 1. Summary of peak wavelengths and energies of CL bands from float glass, silica and quartz

Green float glass eV	Clear float nm	Clear float eV	Silica and quartz eV
1.62	765.00		
1.71	725.00	1.73	
1.91	650.00		1.91
1.98	625.00	1.97	1.95
2.21	562.00		
2.32	535.00	2.31	2.28
2.35	528.00		
2.43	510.00		2.46
2.67	465.00	2.68	2.69
2.82	440.00	2.80	2.72
2.97	417.00		2.93
3.10	400.00	3.10	3.12
3.37	368.00	3.31	
3.68	337.00	3.60	
3.84	323.00		
4.05	306.00		
4.15	299.00	4.14	

Values cited are from Stevens-Kalceff and Phillips (1995) for silica and quartz; Townsend *et al.* (1998) for clear glass, and new data for the green glass.

data (as a linear function of wavelength with a constant wavelength bandpass) and conversion to intensity in terms of an energy axis and constant energy bandpass, there are major changes in the appearance of the data. To emphasise this fact, Fig. 2 shows uncorrected original data for successive spectral scans of a green float glass sample. It is apparent that even for a low beam current of  $\text{nA}/\text{cm}^2$  the short wavelength signals are degraded. The same pattern of behaviour was seen in many samples but the details differ with temperature and the intensity reductions are most apparent for the tin side of the green glass at low temperature. The signals from the non-tin side are somewhat more stable. Conventional current densities are much higher and the time dependence of the signal intensity will be hidden. Nevertheless, comparisons between even such basic data assist in separating the presence of different component features. Similarly, changes in the spectra with temperature reveal the changing importance of the components. In Fig. 3, uncorrected data, normalised at 510 nm, of a green glass sample are shown as a function of temperature. This normalisation emphasises how there is a temperature dependent change in

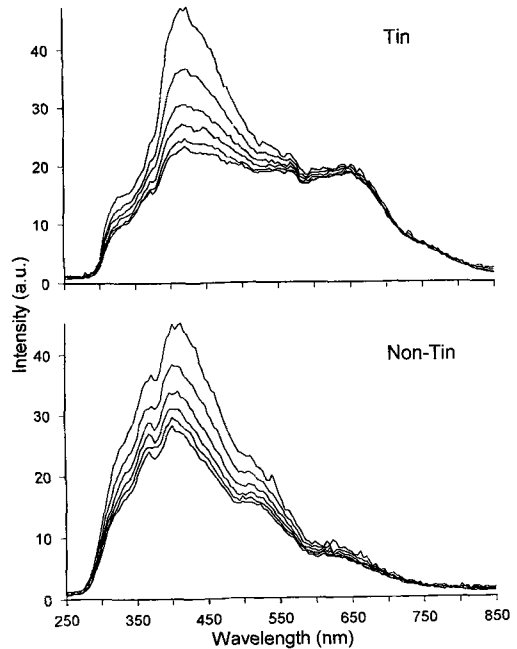


Fig. 2. Uncorrected original data for successive spectral scans of a green float glass sample made at 22K. Even for a low beam current of  $\sim 20 \text{ nA}/\text{cm}^2$  the short wavelength signals are degraded. Conventional current densities are much higher and the time dependence of the signal would normally be hidden.

balance between the short and long wavelength signals. In both Figs. 2 and 3 signals are contrasted from the tin contact surface of the float glass and the upper face (which only receives tin by vapour transport). The basic patterns are similar in terms of damage or temperature but the presence of tin enhances emission from the bands near 600 nm.

Figures 2 and 3 indicate that uncorrected data are valuable in assessing the number of component features, by contrasting samples and recording difference spectra. The green glass is made by addition of iron and this generates at least two emission bands near 725 and 765 nm (attributed to  $\text{Fe}^{3+}$ ). Emission in the long wavelength region for  $\text{Fe}^{3+}$  is reported in many other materials which contain iron. Quartz examples include data by Pott and McNicol (1971) and Gorobets *et al.* (1989), amethyst (Zhang *et al.*, 1994) and there are numerous references listed by Krbetschek *et al.*, (1998) for similar emission from iron in feldspars.  $\text{Fe}^{2+}$  has

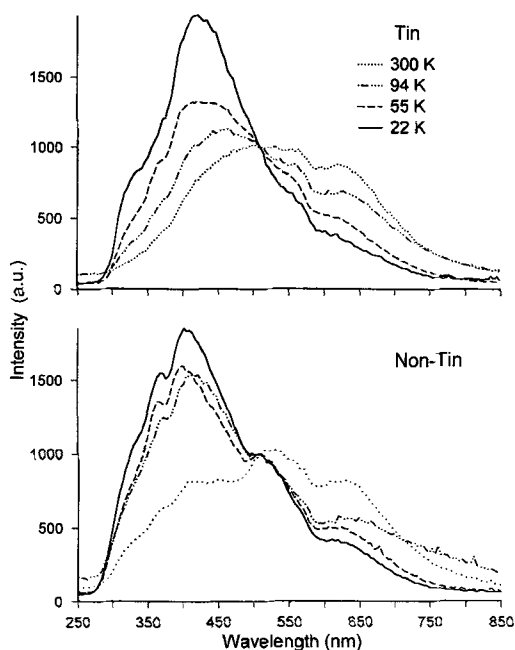


FIG. 3. Comparisons between spectra of green glass taken at different temperatures, and normalised at 510 nm to emphasise the changing importance of short and long wavelength signals.

been suggested as the origin of a luminescence near 550 nm in some silicate minerals. Hence, it may be related to bands near 562 or 528 nm seen in the present detailed analysis for the green glass.

For normal broad band emission features, even for a wavelength presentation of the results, it is essential to correct for the overall efficiency of the system, which invariably is far superior in the blue compared with that in the red region. The systems in Sussex differ variously by up to a factor of 200:1 in blue to red (400 to 800 nm) sensitivity. This wide dynamic range is caused by falling red efficiency of PM tubes and the blaze wavelengths of the diffraction gratings. Energy conversion will of course further exacerbate this sensitivity problem by a further factor of 4. Consequently many groups correct data for system response only in terms of wavelength, and many of the examples shown here will be similarly displayed.

Separation of the component bands can be aided by recording the differences in lifetimes, for example using a lock-in amplifier, or via a more modern version including phase tuning for post

collection phase analysis (Gorton *et al.*, 1999). Figure 4 plots spectra taken with frequencies increased in logarithmic increments from 9 to 30 000 Hz. It is apparent that the various emission bands differ in their decay rates, and several lifetime components must exist, which for this frequency range implies values from tens of msec to less than  $10^{-5}$  s. For the tin face the dominant signal, as for Fig. 1, is near 600 nm, whereas for the non-tin face the strongest emission is in the short wavelength range. The lock-in amplifier recording over a range of frequencies also reveals some unusual characteristics of the excited electron decay routes. For signals near 3.2 eV (390 nm) there is an apparent minimum emission intensity for modulation of 3 kHz, as the signal here is  $90^\circ$  out of phase with the excitation. Interpretation of such an effect requires the luminescence decay process to have proceeded by at least two steps in order to introduce anti-phase emission and a delay of  $\sim 3 \times 10^{-4}$  s.

Decreasing the temperature to 22 K has the effect of resolving some of the component bands, varies their relative intensities, and causes alterations in their decay lifetimes, as is seen by comparisons of Figs. 4 and 5. The complexity of the situation is apparent since nominally the same emission bands have different lifetime behaviour when excited from the tin and non-tin sides of the glass. Similar types of changes are apparent for the green glass samples.

Within the tin side of the float glass there are changes in component CL signal intensities with depth, and these variations have been compared for the same samples with both ion beam analyses of composition (using Rutherford Backscattering Spectrometry, RBS, and Particle Induced X-ray Emission, PIXE), and refractive index data obtained by measurement of optical waveguide modes that are supported by the increased index in the tin face (Townsend *et al.*, 1998). Additional depth information is available from the published analyses using Mössbauer measurements of the  $\text{Sn}^{2+}$  and  $\text{Sn}^{4+}$  variations (Williams *et al.*, 1997). Figure 6 shows that in some cases one may confidently associate the CL intensities to specific ions or valence states. For example, the depth profile of the tin signal, seen by RBS, follows the same pattern as for the strong emission band at 1.97 eV (629 nm), and both the Sn RBS and the 2.68 eV (463 nm) emission show maxima at depths after some 12  $\mu\text{m}$  had been removed from the surface. The buried signal maxima are

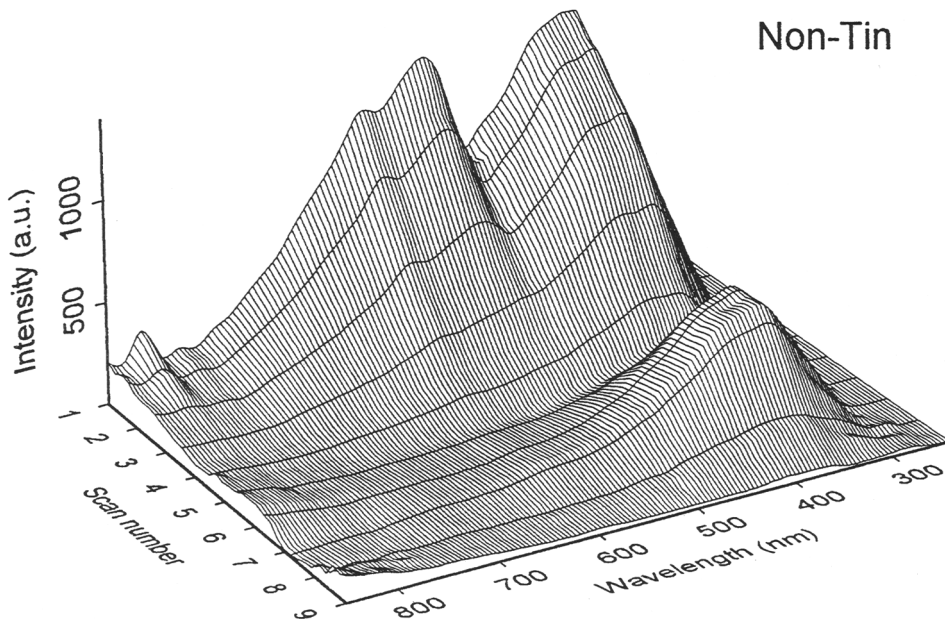
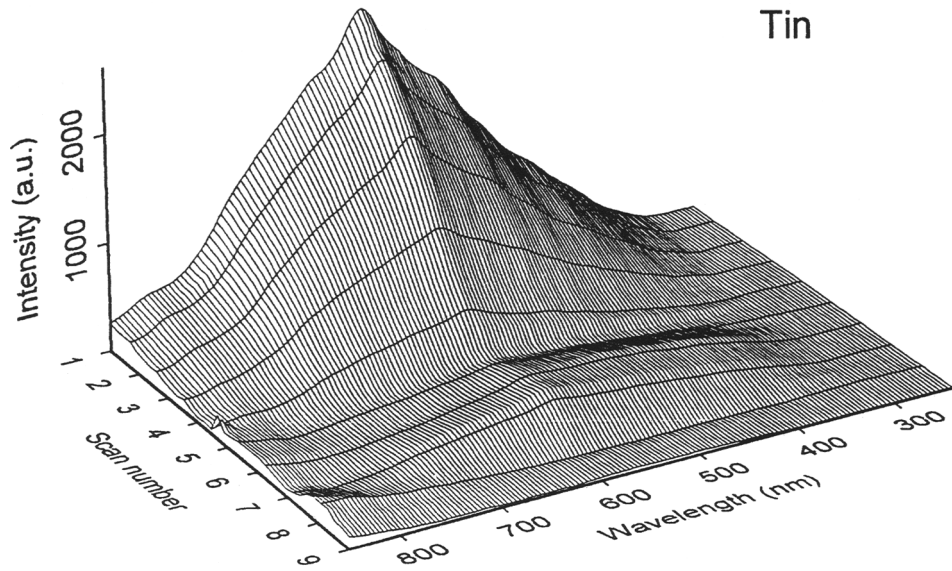


FIG. 4. Room temperature CL spectra of clear float glass obtained using a lock-in amplifier. Note the use of a logarithmic frequency axis with scan numbers corresponding to 9, 30, 90, 300 etc Hz. The spectra are corrected for the efficiency variations of the optical system. Data for the tin and non-tin sides of the glass are shown. The electron energy used was 10 kV.

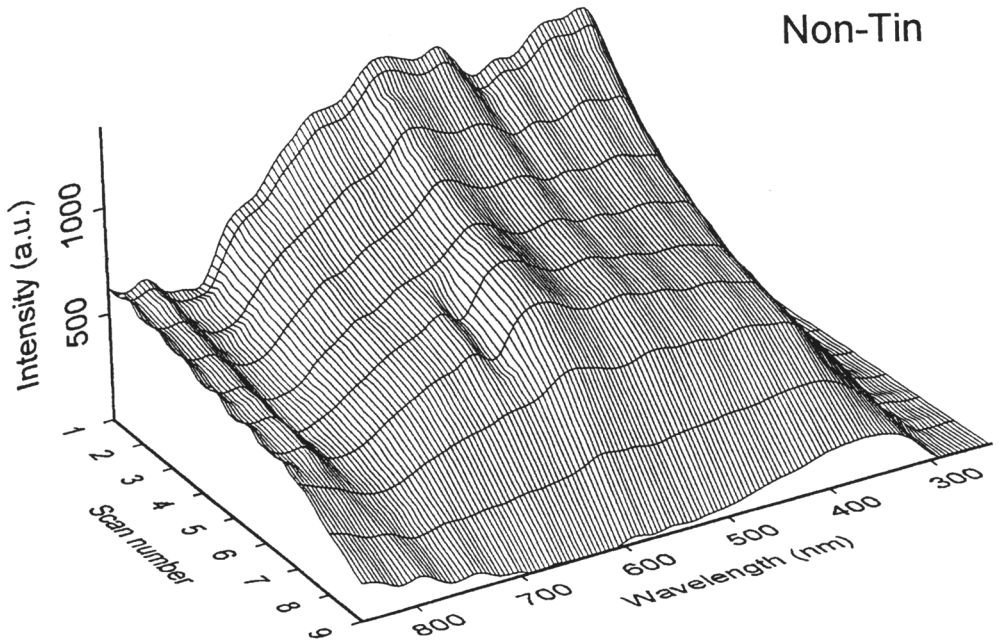
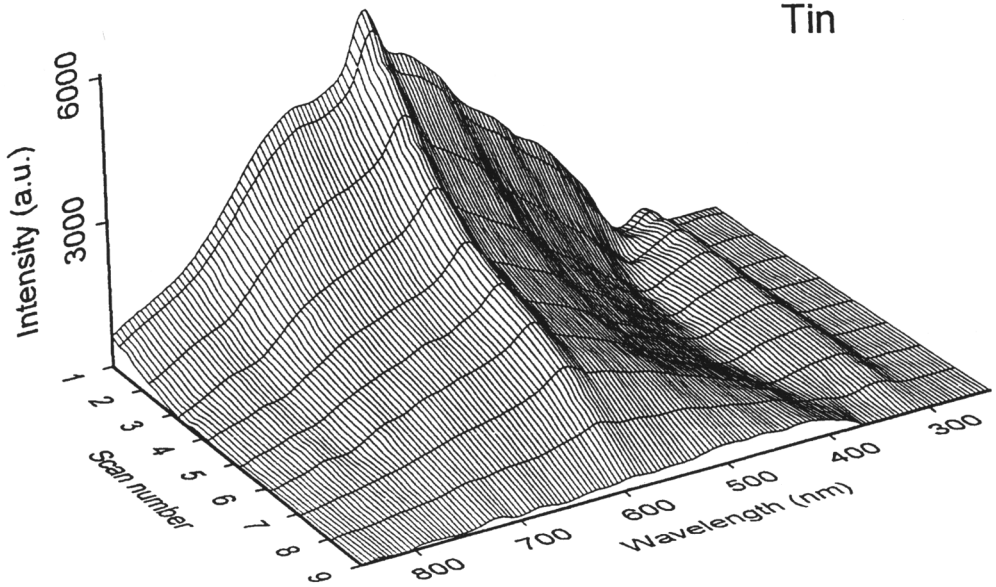


Fig. 5. As for Fig. 4, but for data recorded at 22 K.

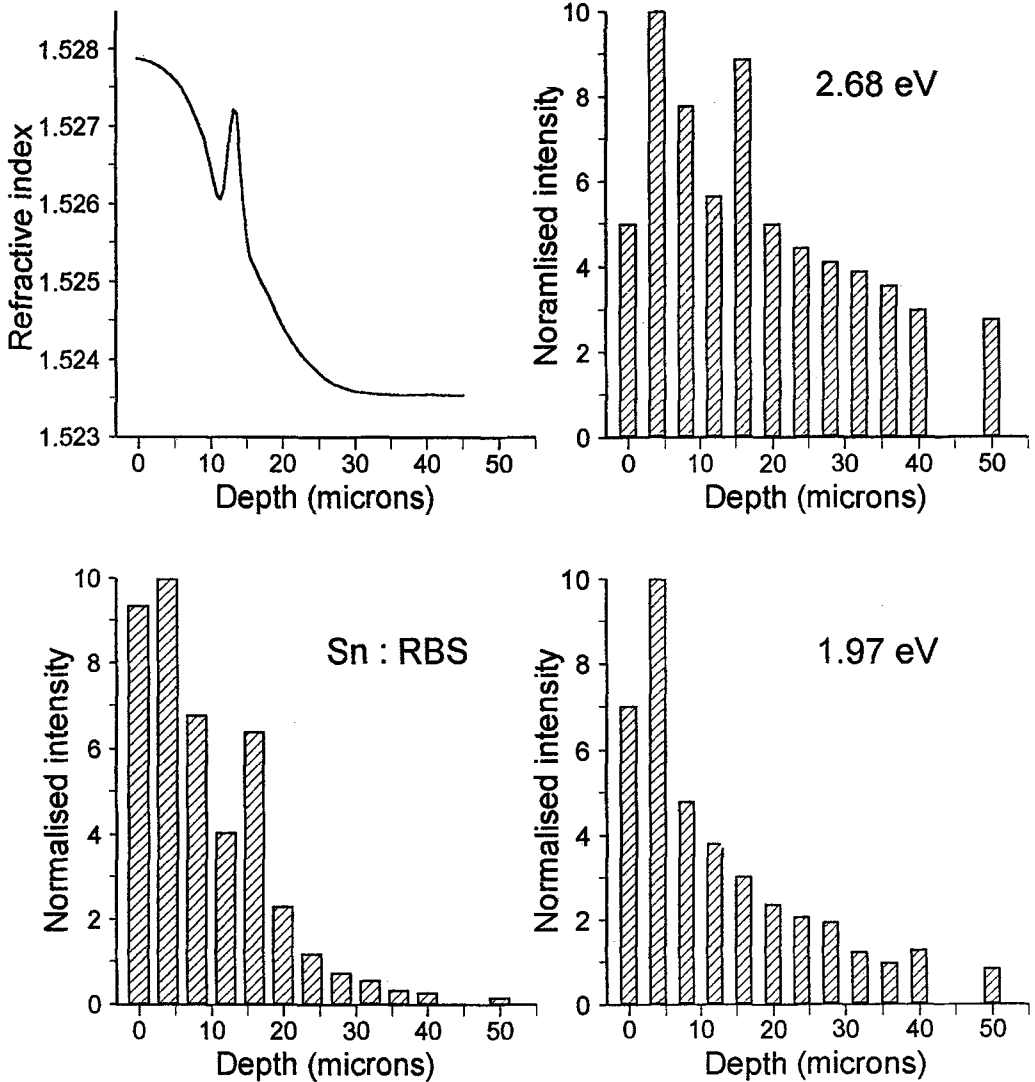


FIG. 6. Comparison of the depth profiles of the total Sn signals seen via RBS, the 1.97 and 2.68 eV emission bands and refractive index profile determined by optical waveguide mode data. Note the waveguide modes do not require sectioning, whilst a polishing sequence was employed for the RBS and CL signals.

also seen very clearly from the waveguide mode analyses, which emphasises that this is not an artefact of the sectioning technique, since the mode analysis is a non-destructive measurement. Mössbauer data indicate a similar buried maximum associated to an increase in the  $\text{Sn}^{4+}$  to  $\text{Sn}^{2+}$  ratio. Therefore the  $\text{Sn}^{2+}$  enhances the production of 1.97 eV CL, whilst the presence of  $\text{Sn}^{4+}$  can be assessed via that at 2.68 eV. It is

important to note that, although there is a strong correlation between the signals and the presence of tin, this does not mean that the tin is necessarily precisely at the luminescence site. Since the same emission is seen in pure silica, it is more probable that the tin has stabilised different intrinsic oxygen vacancy sites (e.g.  $E'$ , peroxy, non-bridging, etc.). The CL to tin RBS correlations are thus consequential rather than direct.

In the case of iron, which can exist in the glass both as  $\text{Fe}^{3+}$  and  $\text{Fe}^{2+}$ , there is broad agreement between the depth profiles seen by PIXE, Mössbauer and EPMA (electron probe micro-analysis). In CL there are at least two infrared bands from  $\text{Fe}^{3+}$  around 1.62 (765 nm) and 1.71 eV (725 nm), and possibly a green feature from  $\text{Fe}^{2+}$  within the bands from 2.21 to 2.35 eV. Unfortunately these are too poorly resolved to define their depth profiles, or record changes in the valence state of the iron.

Direct defect association of the remaining CL bands is more difficult but a consistent pattern appears if one assumes that the high photon energy bands are primarily from decay of relaxed electron-hole pair states (i.e. effectively equivalent to relaxed exciton states), whereas the bands in the range 1.91 to 3.1 eV (649 to 400 nm) arise from transitions at oxygen vacancy defects. This assignment differs from that of some other authors, but reference to the many review articles only emphasises that virtually none of the optical luminescence and absorption bands have been confidently attributed to detailed specific defect site models, and even for the more structurally specific EPR measurements, the defect models are only first order estimates.

### Glass preparation for ZBLAN optical fibres

In attempts to produce optical fibres which can operate at longer infra-red wavelengths than the normal germano-silicate material there has been interest in producing very high purity metal fluoride fibres. Their metallic content of ZrBaLaAlNa leads to the generic name of ZBLAN (Aggarwal and Lu, 1991). However, this highly reactive fluoride glass can be contaminated from the Pt crucibles, and hence a contactless melt process has been developed in which the molten glass is levitated by a gas film (Granier and Potard, 1987). Whilst this solves problems of contamination from the crucible it does not guarantee that the material will be totally homogeneous, or that there will not be intrinsic defects or microcrystallites. Therefore, in parallel with other measurements to quantify such problems, luminescence data were compared for standard melt and levitated ZBLAN glass (Yang *et al.*, 1997). These indicate that adequate luminescence signals could be obtained and overall the study showed there were consistent and quantitative differences between the two types of material. As for most wide-band gap

insulators, the spectra were dominated by bands in the UV/blue spectral region. These, as with the silicates, are assumed to be the result of relaxed electron-hole recombination. The presence of impurities modified the intrinsic transitions and extended the emission to longer wavelengths. In some cases low temperature CL signals were only apparent in the Pt contaminated crucible samples. More intense luminescence was caused by the presence of microcrystallites, which is consistent with data seen for many other materials (e.g. silica glass or crystalline quartz and amorphous YAG, as discussed later). There was also a pronounced difference in the temperature dependence in the CL and radioluminescence efficiencies between the levitated and crucible glasses. In some examples the crucible glass showed anomalous discontinuities in CL intensity which were tentatively interpreted as evidence for crystalline inclusions and/or the presence of platinum from the crucible. Similar evidence for crystalline inclusions appeared from the low temperature spectrally resolved TL of fibres drawn from the boules. Overall, luminescence offered a direct insight into the quality of the material, without the need to proceed to fabricate and measure ZBLAN fibre, which in itself requires very considerable effort to separate fabrication problems from those induced by the starting material.

### Concentration effects on emission wavelength and intensity

Identification of specific luminescence sites, or indeed an imperfection, in an insulator is extremely difficult since, although the structure is normally discussed in terms of the immediate shell of neighbouring ions, the reality is that there are long range interactions which can be sensed over tens of ion shells. In some cases the long range interactions alter the luminescence efficiencies and lifetimes, in others, the structural distortions result in pairing, or precipitation of colloids, nanoparticles or impurity phases. Whilst CL emission is sensitive to the environment around the core of the emission site, it is often extremely difficult to use the data to interpret the details of the ionic arrangements near the luminescence sites. For example, as with the float glass and ZBLAN examples, there are obviously many emission sites and the band widths and lifetimes, etc. alter with changes in concentration and variations in impurities. A consequent problem is that luminescence data

are rarely quantitative. In particular, there is a concentration versus dose dependence which describes a maximum luminescence output corresponding to impurity concentrations of around 0.1 mol.% (i.e. 100 to 1000 ppm). The reduction in light emission at high concentrations results from long range interactions, or pair and cluster formation. Such data are well documented for thermoluminescence dosimeters (TLD) where rare earth ions of Dy or Tm are used to sensitise the TL signals from  $\text{CaF}_2$  or  $\text{CaSO}_4$  (e.g. McKeever *et al.*, 1995). A similar impurity dependence is shown in Fig. 7 in which the TL light intensity from the Mn impurity emission band of calcite is plotted as a function of the total impurity content of  $\text{Mn}^{2+}$ ,  $\text{Pb}^{2+}$  and  $\text{Fe}^{3+}$  (Calderon *et al.*, 1996). It is tacitly assumed that such a plot could be used as the basis for quantitative calibration of other samples, but as is evident from the TL results, the dependencies differ for the three TL glow peaks. Calibration problems arise for at least two reasons. Firstly, if the signal is derived from high dopant concentrations, then any process which can dissociate pairs, (or cause clustering, etc), will raise (or lower) the

emission intensity. Secondly, particularly for CL, there may be luminescence quenching from surface states which override the basic bulk processes. Activation of an increased fraction of the dopant ions may require that the material is not in thermodynamic equilibrium, and so the intensities may change with thermal or electron beam excitation (i.e. during the CL measurement). There are numerous examples of such changes, and an example (Holgate *et al.*, 1994) shows changes in intensity and emission spectra of the TL of Nd doped  $\text{CaF}_2$ , in which slow or rapid furnace cooling of the material leaves the Nd as isolated or associated ions. Slow cooling introduces clustering and a non-radiative decay mechanism for some of the Nd transitions. More rapid pulse heating effects, using laser pulses, can activate greater TL emission from Tm in Tm: $\text{CaSO}_4$  TLD material, which is accompanied by changes in the emission spectra (Karali *et al.*, 1998).

Figure 8 demonstrates some very dramatic improvements in CL intensity which can be produced in highly doped material by pulsed laser annealing. This signal enhancement is not

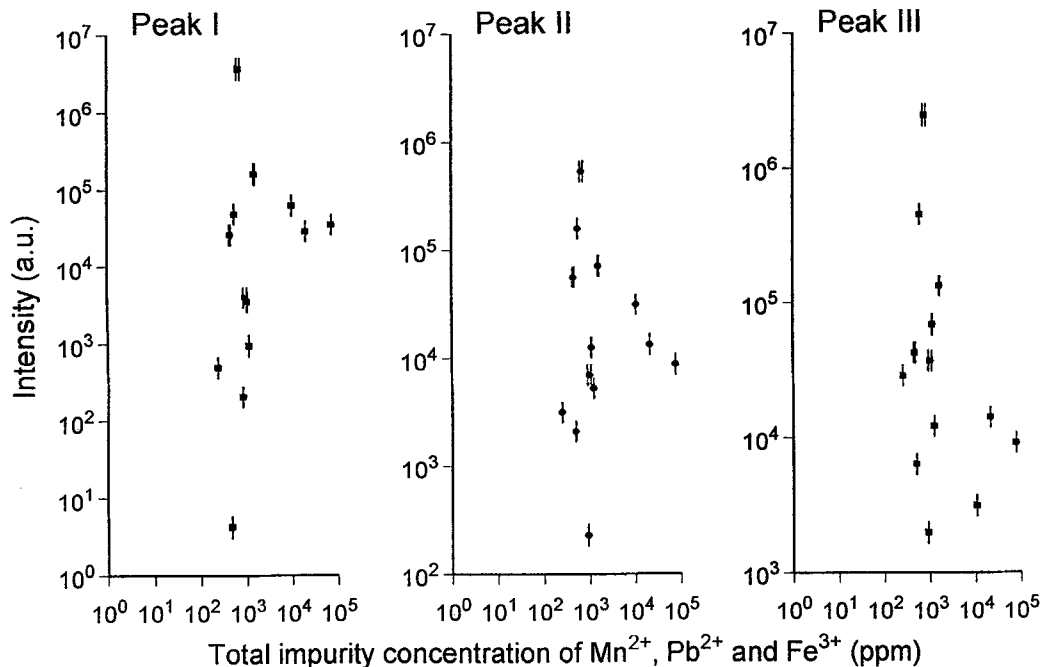


FIG. 7. Influence of impurity content on the intensity of three TL glow peaks in calcite. Note the responses are different for the three trapping sites.

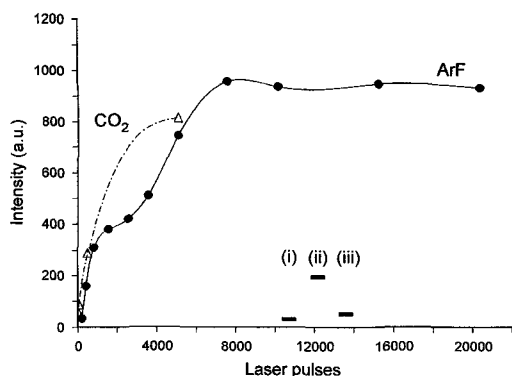


FIG. 8. The influence of pulse laser anneals on the CL intensity from silica implanted with Eu ions. Data for signal improvements caused by furnace anneals are shown by the inset bar lines, where (i) was the original intensity after implantation and (ii) and (iii) correspond to anneals at 1000 and 1200°C.

feasible with furnace treatments. In this work (Can *et al.*, 1995) the dopant Eu ions were implanted into the surface layers of sapphire or silica glass. However, the implantation introduces many intrinsic defects which cause non-radiative decay, and so some thermal annealing process is essential to activate the Eu luminescence. Furnace heating to ~1000°C makes considerable improvements in intensity, shown here in the central inset as levels (i) directly after implantation, and (ii) after 1000°C annealing, but removal of the more stable host lattice defects requires heating to >1200°C. Unfortunately, the high ionic mobility needed to remove damage also allows the Eu ions to migrate and form non-radiative precipitates (evidenced by transmission electron microscopy), and the emission intensity then falls to the value shown by line (iii). By contrast, pulsed laser annealing using either excimer or CO<sub>2</sub> laser pulses (of up to 20 ns duration), removes the intrinsic lattice damage, dissolves and separates pairs or clusters, and since the layer cools to below 1000°C in a few nanoseconds, results in a non-thermodynamic but high concentration of isolated ions. As shown in the figure the final CL line intensities from Eu are some 100 times greater than those achievable by furnace treatments. There are corresponding increases in the Eu excited state lifetime from 2 to 5 ms in silica.

This Eu example is for ion implanted material intended for a surface waveguide laser, but clearly this type of pulse laser surface processing could

be applied much more widely, and is of direct relevance to cathodoluminescence studies since they are sensing signals from the same depth scale below the surface as can be modified by pulse laser annealing. One should therefore consider and explore the benefits in sensitivity which might be obtained by pulse laser annealing of more conventional CL samples.

### Lattice parameter and wavelength shifts of Mn luminescence in carbonates

In cases where the luminescence originates at highly localised lattice sites, such as internal transitions within rare earth ions, chromium ions in ruby or manganese ions in carbonates, then the precise energy of the transition is sensitive to the interaction with the local lattice. The energy (or wavelength) of the emission is thus sensitive to pressure, temperature, and any changes in crystal field caused by the presence of other structural defects or impurity ions. The interactions with these neighbours also modifies polarisation, and relative transition intensities of the component emission lines. Wavelength changes for the ruby example has been documented for more than 70 years and there is also an extensive literature for Mn in a variety of calcite lattices, together with Mn data for other minerals. In carbonates the dominant broad band orange emission has a wavelength movement which correlates well with the length of the metal-oxygen bond in the lattice. Indeed, even in structures with alternative metal ion sites, such as dolomite, one observes two strong emission bands, with intensities proportional to the site occupancies. The configuration co-ordinate diagram of the Mn transitions in calcite includes numerous luminescence possibilities, some of which are at virtually the same wavelength, near 600 nm, as the one assumed to correspond to decay from the lowest excited state. The relative intensities of these component features appear to differ with Mn concentration and thermal treatments of the calcite, hence the identification of the strongest CL peak intensity with transitions between the lowest pair of Mn energy levels could be in error. Nevertheless, if one includes several of the stronger emission lines it is possible to discern a pattern of line movement with lattice parameter. Figure 9 presents data for the wavelength dependence with metal-oxygen lattice spacing (Calderon *et al.*, 1996). Values derived from RL and TL of carbonates show two clear trend lines,

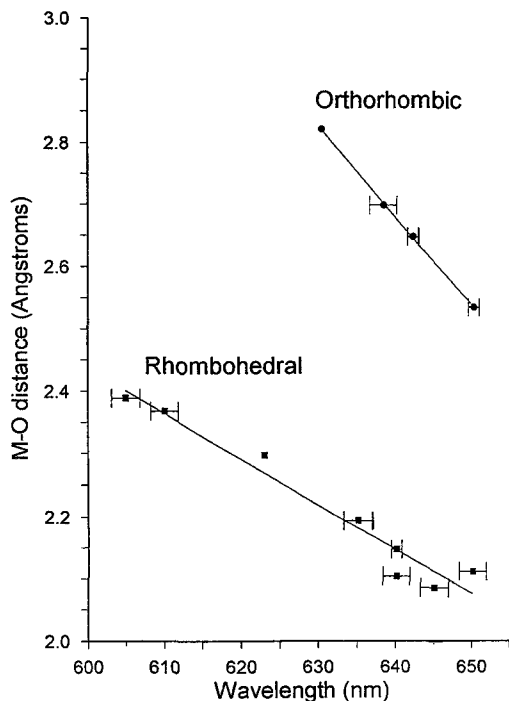


FIG. 9. The wavelength dependence of luminescence from Mn in various carbonate lattices as a function of metal-oxygen spacing. Data are for TL and RL. CL emission has many more bands but the same trends are noted.

corresponding to rhombohedral and orthorhombic lattices. For CL data of these materials earlier results indicated an apparent trend which was totally different. However, the problem is that the CL introduces a variety of strong emission signals and it is no longer obvious that the same transitions are being compared, but if one plots a diagram which includes the many more strong emission lines seen by CL, compared with RL or TL, then this encompasses the same trend as for the RL and TL data. It is important to note that both RL and TL can be derived from the bulk lattice, with only minor perturbations from surface effects, whereas CL is totally dominated by surface distortions and modifications of the chemistry of the lattices. In the absence of the bulk data it would be extremely difficult to know how to compare equivalent Mn energy level transitions in different carbonates. To emphasise this problem, Fig. 10 plots the CL emission spectra from three samples of aragonite taken

from the same block of material. The figures obviously include the same set of orange lines near 2.2 eV (564 nm), which are normally attributed to the presence of Mn. Mn transitions can be assigned to each emission line, but they differ greatly in their relative intensities between samples. Such differences can be exacerbated if the detector systems are polarisation sensitive and single crystals are compared under different orientations.

Overall, for a controlled set of samples, it is possible to monitor the Mn wavelength shifts and link these to a particular host lattice structure, but considerable caution is required if only CL data are interpreted.

### The CL of Nd:YAG surfaces: effects of surface preparation

Rare earth ions are excellent probes of changes in the local crystal field since their CL spectra include transitions which range from highly excited states, from energy levels with orbitals that overlap widely with the neighbouring ions, to well shielded inner levels that are less perturbed by the crystal field. Consequently there are wavelength shifts caused by changes in their environment and alterations in the relative line intensities. Line broadening or relative intensity changes are thus monitors of structure even when the line movements are difficult to record. The presence of grain boundaries and dislocations generally cause considerable reduction in luminescence intensity. Luminescence can be totally quenched in the region of a dislocation line, which has advantages for mineralogical studies, where component grains and zoning effects can be clearly delineated. By contrast, luminescence quenching by dislocations and surfaces is distinctly a problem when trying to maximise luminescence intensity as for CL phosphors or in modern photonic systems of waveguide lasers. The presence of dislocations within the waveguides additionally act as scattering and absorbing centres which increase transmission losses and so degrade the waveguide performance. They may also reduce efficiency of other surface properties, for applications such as electro-optic waveguide modulation, second harmonic generation using the non-linear properties of crystals, or surface acoustic wave interactions, etc. Epitaxial growth is also degraded by the presence of dislocations. Optical waveguides can be fabricated by many methods including ion exchange, chemical

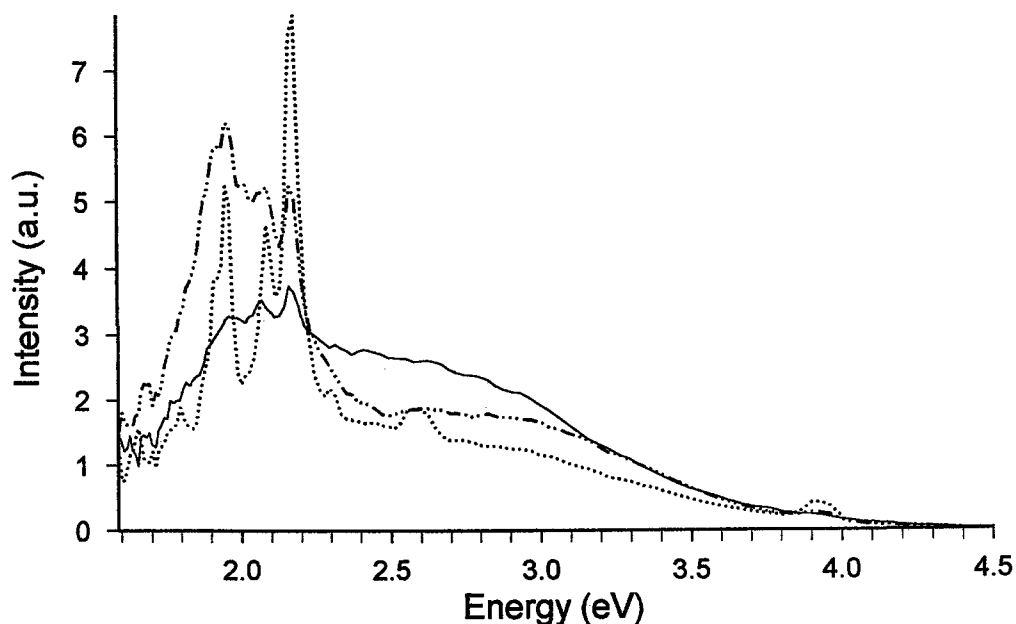


FIG. 10. Three examples of CL of aragonite which show different relative intensities between the component line features. The signals originate at transitions within Mn impurities.

doping, ion implantation of impurities, or ion beam production of a low refractive index damaged layer acting as an optical barrier buried below the waveguide zone. In all cases the waveguide losses are considerably more than those exhibited by bulk materials. For waveguides formed by the latter process in Nd:YAG the laser pump threshold power seems to depend on the quality of the surface polish, therefore we are attempting to correlate the losses with the presence of dislocations and surface damage. In particular, with defects which are generated by the process of cutting and polishing. A second objective is to then find methods which remove the damage, so as to have losses as low as those of bulk material.

Cathodoluminescence is well suited to such studies since for Nd:YAG the presence of dislocations and polishing damage will be reflected both by reductions in the luminescence efficiency, and potentially, by movements of the Nd line emissions. Further, variations in electron energy should probe to different depths into the polished layer. However, the interpretation of the wavelength shifts as a function of electron energy is rather indirect since the signals are a convolution of the energy deposition function, damage controlled luminescence efficiency, and

overlap of the signals from each depth. In practice Nd:YAG is amenable to such analysis. After standard polishing of a Nd:YAG crystal the CL spectra not only change in intensity, but also show movement of the Nd line emissions as a function of the CL electron beam energy. When using high energy electrons (>30 keV) the spectrum closely resembles that seen by RL, i.e. it is then representative of the bulk crystal. CL spectra obtained from different parts of the same surface are not identical and can be seen to correlate with differences in the quality of the polishing. Figure 11 compares spectra taken from different regions of the specimen under identical CL conditions, where the sample had been cut from a large laser boule. The upper curves show the effects of different electron penetration depth, and the lower figure contrasts the better polished central zone with signals from nearer the edges of the sample. Changes in overall intensity and relative line intensity are immediately obvious, and closer inspection indicates small changes in the peak positions, which are greatest from the less well polished regions. Figure 11 emphasises changes in relative intensity and overall CL signals are weaker from the poorly polished material, but it is necessary to specify the wavelength in order to quote the precise decrease

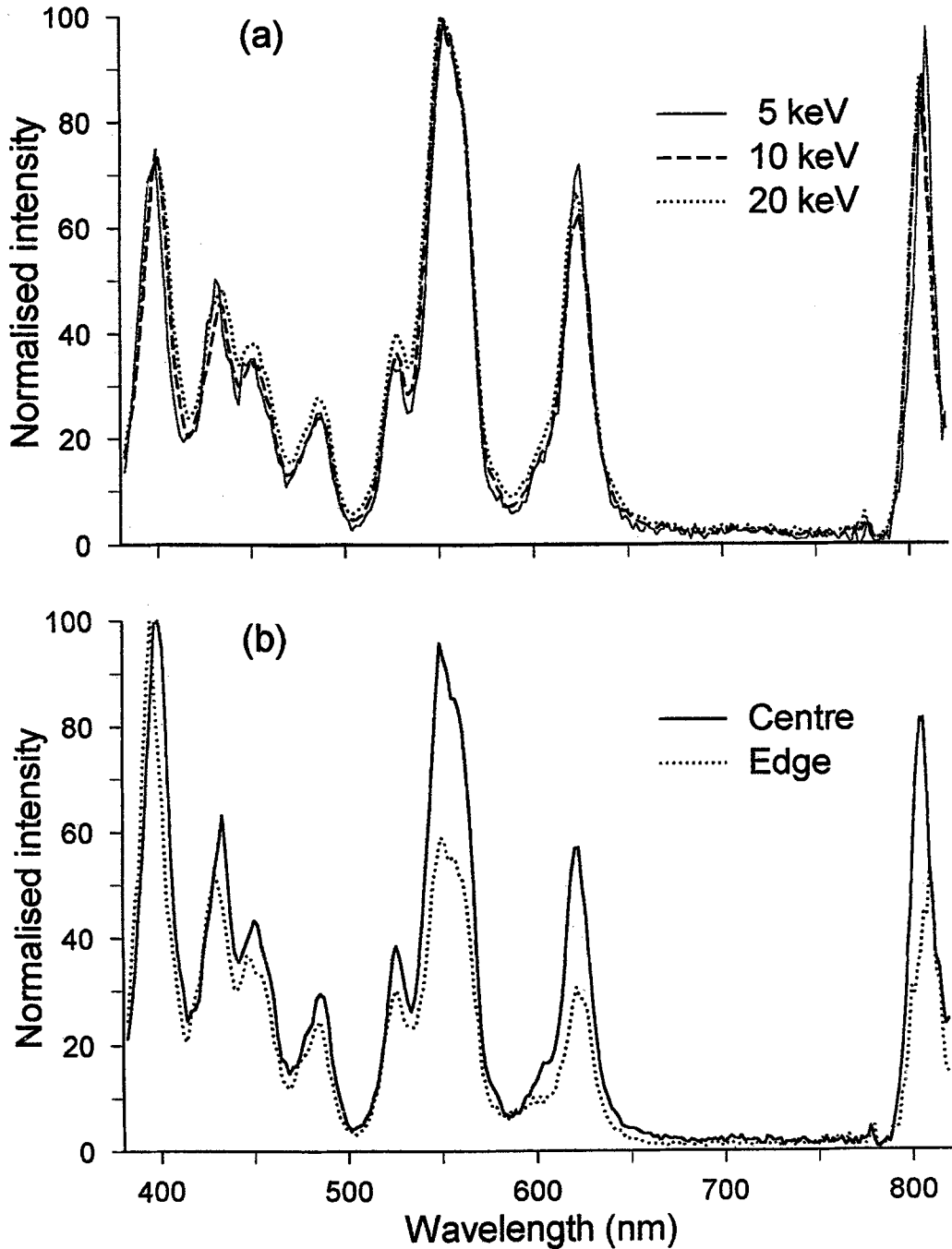


FIG. 11. (a) CL spectra from the surface of Nd:YAG produced with 5, 10 and 20 keV electrons, in order to emphasise either surface damage or signals from the bulk material. (b) A comparison of spectra from a central well polished zone with one from the edge region where there is a higher density of scratches and polishing marks.

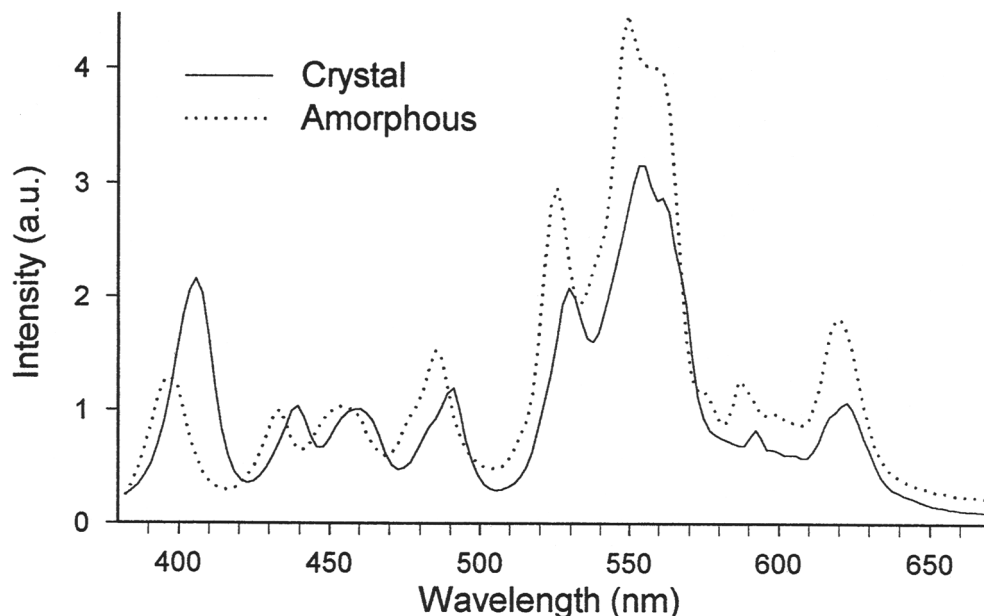


FIG. 12. Low resolution spectra of Nd:YAG which contrast the emission pattern from bulk crystalline material (solid line) with the CL from an ion beam amorphised surface layer. Note the damaged material differs in spectral detail and is reduced in intensity by  $\sim 1000$  times.

in intensity caused by the presence of dislocations. The surface damage shifts the envelope of the shorter wavelength lines to even shorter wavelengths. By contrast the lines near 805 nm emphasise the longer components in the damaged zone. Figure 12 shows that, even with a low resolution spectrometer, there is a clear difference in wavelength between signals from the bulk material and a damaged surface layer and for this demonstration the damage to the crystalline YAG lattice has been maximised by amorphisation with a neon ion beam. The consequent CL intensity is reduced by  $\sim 1000$  times (Peto *et al.*, 1997).

To correlate CL features with dislocation effects the dislocation density has been revealed by chemical etching with orthophosphoric acid, and then the line density measured using a scanning electron microscope (SEM). The typical density was  $\sim 10^5$  dislocations per  $\text{cm}^2$ . The etching also caused an enhancement in the CL intensity, presumably by removal of highly damaged material that quenched the luminescence. In order to remove the damage layer totally, the polished surface was ion beam damaged to increase the chemical etch rate. Chemical attack of this modified surface is most

instructive since, as shown in this SEM (Fig. 13), the apparently well polished flat surface, seen in the upper part of the picture, hides a tangled mass of scratch and polishing damage stress lines.

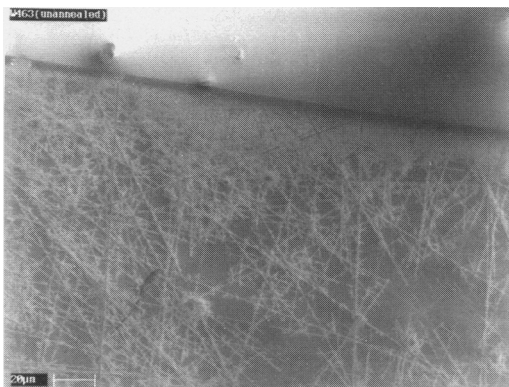


FIG. 13. An SEM photograph of the surface of Nd:YAG after polishing and chemical etching. The upper 'smooth' zone is as polished and the lower region has been exposed to ion beam damage to enhance the chemical etch rate and so reveal the true extent of the damage and stress lines caused by the polishing.

A few deeper scratches traverse both the protected and damaged/etched zones. Finally, high ion beam doses totally amorphise the surface and so destroy the dislocation lines and any preferential etching. Amorphised YAG etches some ~700 times faster than the original crystalline YAG (Nunn *et al.*, 1997), a feature seen with other garnets as well. After several amorphisation and etch cycles the entire layer which had been influenced by the cutting and polishing was removed. In the present example this corresponded to a depth layer of between 1 and 2  $\mu\text{m}$ . The resultant new surface had the flatness and optical quality of the starting material, but the dislocation density fell to ~10 per  $\text{cm}^2$ , i.e. an improvement of  $10^4$ .

The CL intensity of this new surface was 250% greater than the original, there were also significant improvements in the quality of the He ion beam waveguides formed in this new surface, with photoluminescence from within the guides being increased by ~40%. Earlier work with bulk Nd:YAG lasers (Gan, 1995) had noted a correlation between dislocation density and threshold pump power where broadly, a factor  $10^2$  reduction in dislocation density corresponded to a factor of 2 in lasing threshold power. Thus for the present example, a laser waveguide threshold power should be improved fourfold.

#### Comments on the method of removal of damage arising from sample preparation

Improved surface quality which is free of dislocations, etch pits, or chemical modification caused by the mechanical preparation techniques of the surface are of great value for all surface dominated optical properties, as for the waveguides and surface structures of developing photonic and opto-electronic applications. They are also of significance for surfaces prepared for subsequent epitaxial layer growth, and for any surface luminescence process such as CL. Changes in surface quality of insulating materials can be readily monitored by CL. The YAG example emphasises that reductions in efficiency of 1000 times can be introduced by damage. This is of particular interest for CL imaging studies as many of the petrological sectioning techniques are extremely aggressive in terms of surface damage and, as seen above, a subsequent polish which produces an optical flat on the outer surface, does not remove the crucial buried damage which extends throughout the zone probed by a CL

electron beam. The use of the post polishing surface removal technique should therefore be beneficial, not only for photonics, but also for many other CL applications. An increased CL intensity would allow use of lower electron beam currents and so minimise heating and damage effects in the sample, and ease the problems of light collection for spectral analysis. It is important to note that garnets are not alone in being chemically more reactive after ion beam amorphisation. Indeed this is a general feature of crystalline materials, and is also seen to lesser extents in ion beam bombardment of glass. Familiar mineralogical examples include amorphisation of quartz to silica glass, and solid state fission track detectors (in both cases the etch rates increase by several hundred times), and even greater changes in chemical reactivity can be triggered by photostimulation of the etchants or the etched surface.

#### Conclusions

This set of examples of CL emphasises some new applications of the method and underlines the value of having spectral information. The analytical power of the CL resides in its sensitivity to changing surface conditions, and when linked to other techniques may lead to more detailed models of the luminescence sites. The improvement in surface quality developed for Nd:YAG has much wider potential, and may be used to improve many surface optical structures and to enhance both CL intensity and analyses.

#### Acknowledgements

We wish to thank EPSRC, for financial support and also The Mineralogical Society for stimulating this review as the result of presenting some of this material in a keynote lecture in the 'Microbeam Techniques in the Geosciences' meeting in January 1998. Finally, we are indebted to Derek Underdown for his considerable skill in crystal polishing.

#### References

- Aggarwal, I.D. and Lu, G. (1991) (Eds) *Fluoride Glass Fiber Optics*, Academic Press, Boston.
- Agullo Lopez, F., Catlow, C.R.A. and Townsend, P.D. (1988) *Point Defects in Materials*, Cambridge University Press, London.

- Calderon, T., Townsend, P.D., Beneitez, P., Garcia-Guinea, J., Millan, A., Rendell, H.M., Tookey, A., Urbina, M. and Wood, R.A. (1996) Crystal field effects on the thermoluminescence of manganese in carbonate lattices. *Rad. Measurements*, **26**, 719–31.
- Can, N., Townsend, P.D., Hole, D.E., Snelling, H.V., Ballesteros, J.M. and Afonso, C.N. (1995) Enhancement of luminescence by pulsed laser annealing of ion implanted europium in sapphire and silica. *J. Appl. Phys.*, **78**, 6737–44.
- Crookes, W. (1879) Contributions to molecular physics in high vacua. *Phil. Trans. Royal Soc.*, **170**, 641–2.
- Gan, F. (1995) *Laser Materials*. World Scientific, Singapore.
- Gorobets, B.S., Gaft, M.L. and Podolskiy, A.M. (1989) *Luminescence of minerals and ores*, Ministry of Geology, Moscow USSR.
- Gorton, N.T., Walker, G. and Burley, S.D. (1999) Experimental analysis of the composite blue CL emission in quartz — is this related to aluminium content. In *Cathodoluminescence in Geosciences*, (M. Pagel *et al.*, eds.). Springer-Verlag, Berlin, (in press).
- Granier, J. and Potard, C. (1987) Containerless processing and modeling materials by the gas film levitation technique: early demonstration and modeling. *Proc. 6th European Symp. on Material Sciences under microgravity conditions*, Bordeaux, France 2–5 December 1986. Document ESA SP-256.
- Holgate, S.A., Sloane, T.H., Townsend, P.D., White, D.R. and Chadwick, A.V. (1994) Thermo-luminescence of calcium fluoride doped with neodymium. *J. Phys. Condensed Matter*, **6**, 9255–66.
- Karali, T., Rowlands, A.P., Townsend, P.D., Prokic, M. and Olivares, J. (1998) Spectral comparison of Dy, Tm and Dy/Tm in CaSO<sub>4</sub> thermoluminescent dosimeters. *J. Phys. D*, **31**, 754–65.
- Krbetschek, M.R., Gotze, J., Dietrich, A. and Trautmann, T. (1998) Spectral information from minerals relevant for luminescence dating. *Rad. Measurements*, **27**, 695–748.
- Marshall, D.J. (1988) *Cathodoluminescence of Geological Materials*. Unwin Hyman, London.
- McKeever, S.W.S., Moscovitch, M. and Townsend, P.D. (1995) *Thermoluminescence Dosimetry Materials: Properties and Uses*. Nuclear Technology Publishing, Ashford UK.
- Merbay, J., Townsend, P.D. and Smith, V.A. (1998) Cathodoluminescence changes resulting from humidity and thermal treatments of float glass. *Proc. Glass Technol. Meeting 1997. In Topical Issues in Glass*, **2**, 73–80.
- Nunn, P.J.T., Olivares, J., Spadoni, L., Townsend, P.D., Hole, D.E. and Luff, B.J. (1997) Ion beam enhanced chemical etching of Nd:YAG for optical waveguides. *Nucl. Inst. Methods B*, **127/128**, 507–11.
- Ozawa, L. (1990) *Cathodoluminescence*, Theory and applications. Kodansha, Tokyo.
- Pagel, M., Barbin, V., Blanc, Ph. and Ohnenstetter, D. (1999) (Eds) *Cathodoluminescence in Geosciences*, Springer-Verlag, Berlin, (in press).
- Peto, A., Townsend, P.D., Hole, D.E., Harmer, S. (1997) Luminescence characterisation of lattice site modifications of Nd in Nd:YAG surface layers. *J. Modern Optics*, **44**, 1217–30.
- Pott, G.T. and McNicol, B.D. (1971) Spectroscopic study of the coordination and valence of Fe and Mn ions in and on the surface of aluminas and silicas. *Disc. Faraday Soc.*, **52**, 121–31.
- Remond, G., Cesbron, F., Chapoulie, R., Ohnenstetter, D., Roques-Carmes, C., Schvoerer, M. (1992) Cathodoluminescence applied to the microcharacterization of mineral materials: a present status in experimentation and interpretation. *Scanning Microscopy*, **6**, 23–68.
- Stevens-Kalceff, M.A., Phillips, M.R. (1995) Cathodoluminescence microcharacterization of the defect structure of quartz. *Phys. Rev. B*, **52**, 3122–34.
- Townsend, P.D., Can, N., Chandler, P.J., Farmery, B.W., Lopez-Herrerredos, R., Peto, A., Salvin, L., Underdown, D. and Yang, B. (1998) Comparisons of tin depth profile analyses in float glass. *J. Non Cryst. Solids*, **223**, 73–85.
- Walker, G. and Burley, S. (1991) Luminescence petrography and spectroscopic studies of diamagnetic minerals. In *Luminescence Microscopy*, (C.E. Barker and O.C. Kopp, eds.).
- Williams, K.F.E., Johnson, C.E., Greengrass, J., Tilley, B.P., Gelder, D. and Johnson, J.A. (1996) Tin oxidation states, depth profiles of Sn<sup>2+</sup> and Sn<sup>4+</sup> in float glass by Mössbauer spectroscopy. *J. Non-Crystalline Solids*, **211**, 164–72.
- Yacobi, B.G. and Holt, D.B. (1986) Cathodoluminescence scanning electron microscopy of semiconductors. *J. Appl. Phys.*, **59**, R1–R24.
- Yacobi, B.G. and Holt, D.B. (1990) *Cathodoluminescence Microscopy of Inorganic Solids*. Plenum Press, New York.
- Yang, B., Townsend, P.D., Can, N., Janke, A., Baniel, P., Blanc, O. and Granier, J. (1997) Luminescence of levitated Zr-Ba-LaAl-Na fluoride glass. *Phys. Rev. B*, **56**, 5876–84.
- Zhang, Q., Yang, B., White, D.R.R., Townsend, P.D. and Luff, B.J. (1994) Thermoluminescence spectra of amethyst. *Rad. Measurements*, **23**, 423–31.

[Manuscript received 21 September 1998]